Detection improvement of unburned carbon content in fly ash flow using LIBS with two-stage cyclone measurement system

Zhenzhen Wang[1,2], Renwei Liu[2,3], Yoshihiro Deguchi[2,1 *], Seiya Tanaka[2], Kazuki Tainaka[4], Kenji Tanno[4], Hiroaki Watanabe[5], Junjie Yan[1,2], Jiping Liu[3]

[1]State Key Laboratory of Multiphase Flow in Power Engineering, Xi'an Jiaotong University, Xi'an, 710049, China

[2]Graduate School of Advanced Technology and Science, Tokushima University, Tokushima, 770-8501, Japan

[3]Moe Key Laboratory of Thermo-Fluid Science and Engineering, Xi'an Jiaotong University, Xi'an, 710049, China

[4]Energy Engineering Research Laboratory, The Central Research Institute of Electric Power Industry, Kanagawa, 240-0196, Japan

[5]Department of Mechanical Engineering, Kyushu University, Fukuoka, 819-0395, Japan

Abstract

Fly ash contents can be considered as a basis for optimal and stable boiler combustion control and fly ash quality control in power plant, especially the unburned carbon in fly ash. The real-time and quantitative measurement of contents in fly ash was studied using a constructed two-stage cyclone measurement system and detected using laser-induced breakdown spectroscopy(LIBS) technique. The surrounding gas effect, such as CO_2 effect on unburned carbon content, was studied comprehensively in this paper. The CO_2 effect was eliminated using this proposed combination method of two-stage cyclone measurement system and LIBS with 1ns pulse-width laser according to the efficient gas-particle separation and the controlled laser-induced plasma processes of particle flow. The quantitative analysis was improved using the plasma temperature correction method with the intensity ratio of the emission pair from magnesium as a plasma temperature indicator. The measurement of unburned carbon content in fly ash with temperature correction method presented the concordant results analyzed by chemical analysis method. It is demonstrated the feasibility and improved detection ability for the real-time measurement of fly ash contents in power plant.

Keywords: laser-induced plasma processes, unburned carbon, CO_2 effect, two-stage cyclone measurement system

1. Introduction

The coal-fired power plants are the main force of the electric power. The prerequisite for optimal operation of multiple coal-fired boilers is the fast and precise measurement of fuel properties and combustion conditions. The contents of fly ash highly depending on the coal quality and combustion procedure are considered as a basis for optimal and stable boiler combustion control and fly ash quality control, especially the unburned carbon in fly ash which is one of the most important indicators to evaluate the combustion efficiencies of boilers and the commercial value of the produced fly ash. Unburned carbon in fly ash is the major determinant of combustion efficiency. However, low-NOx technologies and other pollution control systems usually produce high level of unburned carbon in fly ash, which will reduce the overall boiler efficiency[1-4]. The utilization remains an effective strategy to prevent landfilling of fly ash, such as the building materials production of cement additive and concrete production, electrospun nanofiber membrane, aluminosilicate for sequestration of aqueous and gaseous pollutants, applications of fly ash for CO_2 capture, utilization, and storage, etc.[5-9]. Therefore, the determination of fly ash contents and properties is very important, especially unburned carbon in fly ash.

Laser-induced breakdown spectroscopy(LIBS) based on the atomic emission spectroscopy is the technique to analyze the composition and concentration of solid, liquid, gas and aerosol materials. Because of its fast response, high sensitivity, multi-elemental detection, real-time and non-contact features and simplicity of LIBS apparatus, LIBS technique has been applied in various fields[10-18]. For example, LIBS technique has been widely applied to analyze the compositional characterization of various coals under different conditions[19-24]. The gross calorific value of coal, the combustion state, the slagging behavior and other property can also be determined according to LIBS measurement[25-28]. In order to overcome the difficulty of direct particle measurement due to the loose feature, particle sample was pressed into solid phase and then measured using LIBS to enhance the measurement accuracy[29,30]. The integrated and fully software controlled LIBS-based coal quality analyzers were designed for possible application to power plants using different sampling equipment[31,32]. As for the fly ash measurement, this group also developed an automated prototype LIBS apparatus comprising an isokinetic sampler, a sample preparation module, and a LIBS module for on-line analysis of unburned carbon in fly ash[33]. Several developed methods were also proposed to measure unburned carbon in fly ash. The molecular CN was adopted to rapidly measure unburned carbon in fly ash by LIBS. The particle flow-spark induced breakdown spectra(PF-SIBS) was employed for the rapid measurement of unburned carbon in fly ash. A series of data processing methods including spectral interference correction and quantitative analysis methods were carried out to improve the measurement accuracy[34,35]. A homemade gas-solid flow generation system was also developed to simulate the gas-solid flow in the duct of a coal-fired plant by this group[36]. LIBS has also been applied to detect the pulverized coal, char and unburned carbon in fly ash without any sample preparation under high-pressure and high-temperature conditions. The correction factors for quantitative measurement were proposed and determined to surpass the calibration difficulty of aerosol sample. This automated LIBS apparatus was also transferred to a boiler-control system of a coal-fired power plant to achieve the optimal and stable combustion[37,38]. The CO_2 effect on unburned carbon was rather sensitive to its concentration and less than 1% CO_2 caused the spurious C signal for unburned carbon in fly ash[38]. The quantitative elemental detection of size-segregated particles, such as coal and fly ash, was studied to clarify the content dependence on particle diameter. The capability for quantitative analysis of particle contents was improved using the plasma temperature correction method by choosing the appropriate temperature correction range[39-41]. Fig.1 shows one schematic diagram of optimal boiler control system using LIBS in actual coal-fired power plant for fly ash measurement. Actually, measurement of fine particles is not only benefit to industrial processes, but also important for the environmental protection and human health aspects. Except for thermal power plant, particles also produce and release from other industries, transportation, etc. Therefore, fine particle measurement is very significant.

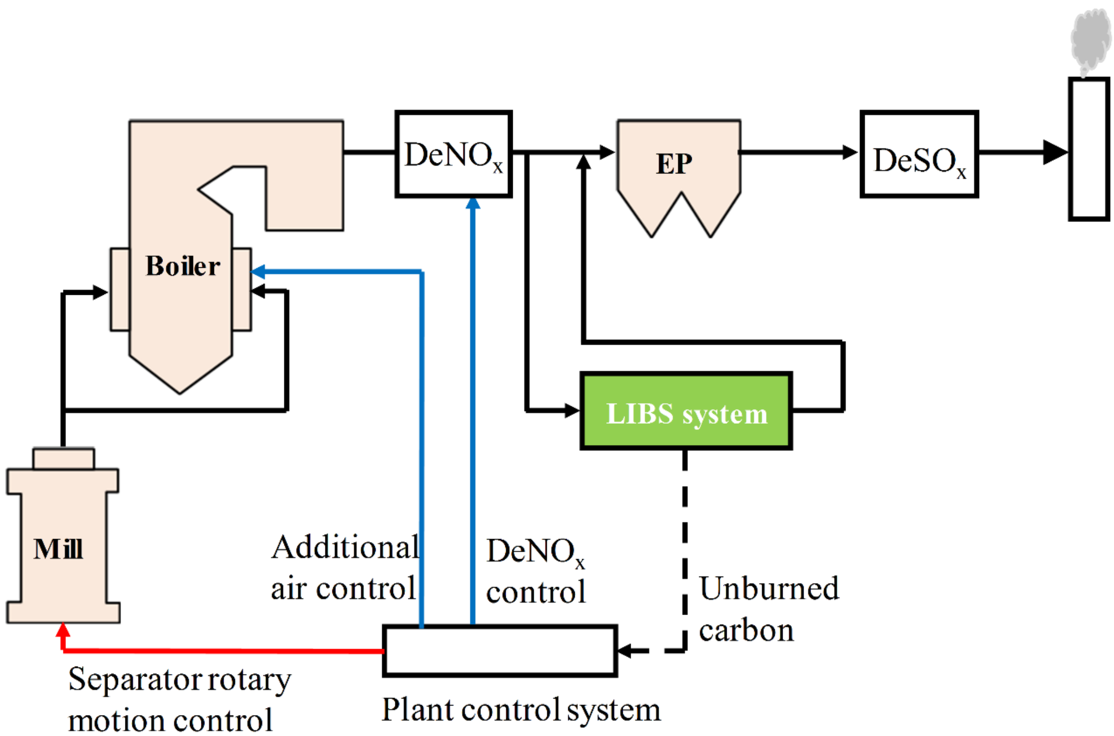

Figure 1. Advanced control system by real-time measurement of unburned carbon in fly ash using LIBS

Plentiful studies have been reported the measurement methods and quantitative analysis methods of unburned carbon in fly ash using LIBS. Influence of surrounding gases and its appropriate diminution approaches, especially CO_2 effect on unburned carbon in fly ash flow, have not been clarified comprehensively. The plasma temperature is also a very important factor for the LIBS quantification. Therefore, the plasma temperature correction is necessary to assure the quantitative measurement, especially for the particle measurement in gases. In this study, the surrounding CO_2

effect and the quantitative analysis method of fly ash contents were discussed to accurately evaluate unburned carbon in fly ash. Two different nanosecond pulse-width lasers were employed here to study the laser-induced plasma processes of particle flow to reduce surrounding CO_2 effect. The developed two-stage cyclone measurement system for fly ash flow was also proposed to reduce the surrounding CO_2 gas effect on unburned carbon content in fly ash.

2. Theory

LIBS technique is based on atomic emission spectroscopy to analyze the material composition and concentration. A laser beam is focused into a small area to atomize material and produce hot plasma. The light emitting from the excited atoms corresponds to a unique wavelength of each element in plasma. The relation between emission intensity and species concentration can be characterized simplistically by the following equation with the assumption of uniform plasma temperature[11]:

$$I_{\mathrm{i}} = n_{\mathrm{i}} K_{\mathrm{i,j}} g_{\mathrm{i,j}} \exp\left(-\frac{E_{\mathrm{i,j}}}{kT}\right) \tag{1}$$

Where, I_{i} is the emission intensity of species i, n_{i} is the concentration of species i, $K_{\mathrm{i,j}}$ is a variable that includes Einstein A coefficient from the upper energy level j, $g_{\mathrm{i,j}}$ is the statistical weight of species i at the upper energy level j, $E_{\mathrm{i.j}}$ is the upper level energy of species i, k is the Boltzmann constant and T is the plasma temperature.

The main elements of fly ash are Si, Al, Fe, Ca and C. The carbon content can be calculated using the emission intensity ratios of Al, Fe, Ca and C to Si that is the main element in fly ash according to the following equation[39,40]:

$$\text{Carbon content} = \frac{\alpha_C I_C / I_{Si}}{1 + \alpha_{Al} I_{Al} / I_{Si} + \alpha_{Fe} I_{Fe} / I_{Si} + \alpha_{Ca} I_{Ca} / I_{Si} + \alpha_C I_C / I_{Si}} \quad (2)$$

Where, α_i is a variable factor related to species *i* and containing the plasma temperature correction factor. These parameters should be determined under the experimental conditions. In equation (1), a uniform plasma temperature is assumed. The plasma temperature intrinsically fluctuates, which causes the calibration fluctuation from LIBS signal intensities. Therefore, emission intensity I_i is a function of species *i* concentration and plasma temperature. A plasma temperature correction method was proposed to improve the quantitative analysis capability of LIBS signal by our group, which was described in detail elsewhere[39,40]. Different emission spectra from the same species are selected as a plasma temperature indicator to correct the plasma temperature dependence of emission intensity. α_i is defined by using the intensity ratio of different emission spectra from the same species with the temperature correction factor. The concentration ratio will become a function of species concentration and does not depend on the plasma temperature. The temperature correction factor theoretically can be calculated using the atomic parameters. However, the laser-induced plasma is non-thermodynamic equilibrium plasma with complex processes. The correction factor depends on the experimental conditions such as the optical setups, pressure, buffer gas composition, etc. Therefore, the correction factor should be evaluated under specific experimental conditions. In this study, the emission intensity ratio of ionic magnesium to atomic magnesium was employed as the plasma temperature indicator for fly ash sample.

In the measurement of particle flow, the breakdown thresholds of gas and particle are different, which result in different laser-induced plasma processes of fly ash particles and surrounding gases. The breakdown threshold of particle is usually lower than that of gas. The laser-induced particle plasma firstly will become the plasma core. During the plasma expending process, the surrounding gas can be induced by the electron collision ionization process. There is the time difference between the particle plasma and gas plasma generation. Therefore, The laser energy and laser pulse width can be altered to control the surrounding gas plasma generation by multi-photon ionization and electron collision ionization to study the surrounding CO_2 effect on unburned carbon measurement in fly ash, especially the laser pulse width[42].

3. Experiment

Fig. 2 illustrates the experimental systems of fly ash measurement using LIBS in this study. A two-stage cyclone measurement system was constructed for fly ash flow measurement, especially for the unburned carbon measurement to eliminate the surrounding CO_2 effect, that is, cyclone 1 and cyclone 2, as showed in Fig. 2(a). Cyclone 3 was utilized to recapture the measured fly ash. The feature of cyclone was detected continuously for a certain period of time after the fly ash flow became stable. Table 1 lists the recaption rate of cyclone in different cases, which were more than 90%. The feeder (Nisshin Engineering Feedcon-μ Mtype) was employed to introduce the fly ash sample into the experimental system by adjusting the rotational speed. The measurement chamber was a cylindrical cell with four quartz windows. The surrounding mixture gas of N_2 and CO_2 was also introduced into the experimental system to form the continuous and steady fly ash flow. Several ejectors were installed to introduce N_2 to maintain the stable flow in this system. Around the input pipe of the measurement chamber, the surrounding gas of N_2 was introduced into the chamber to stabilize the fly ash flow in chamber. The fly ash flow with the surrounding mixture gas of N_2 and CO_2 was also directly introduced into the measurement chamber, as shown in Fig. 2(b), to clarify CO_2 effect on unburned carbon measurement. The measured fly ash particle samples with different unburned carbon contents were provided using a coal-fired furnace as the practical samples. The contents of different fly ash samples analyzed using the chemical analysis methods (Japanese Industrial Standards JIS-M-8801, JIS-M-8815) were listed in Table 2. Fig. 2(c) shows one picture and particle size distribution of fly ash sample. The fly ash sample with unburned carbon of 24.9% was measured using the two-stage cyclone system and the direct measurement system of fly ash flow to discuss the CO_2 effect on unburned carbon content when introducing different CO_2 concentration and utilize different pulse-width lasers. Different fly ash samples were measured using the two-stage cyclone system of fly ash flow to quantitatively analyze the fly ash contents with the temperature correction method.

Table 1. Cyclone recaption rate

Number	Feeder input (g)	Captured ash (g)	Recapture rate(%)
1	4	4	1.00
2	4.2	3.9	0.93
3	4.4	4.2	0.95
4	4.4	4.4	1.00
5	4.5	4.6	1.02

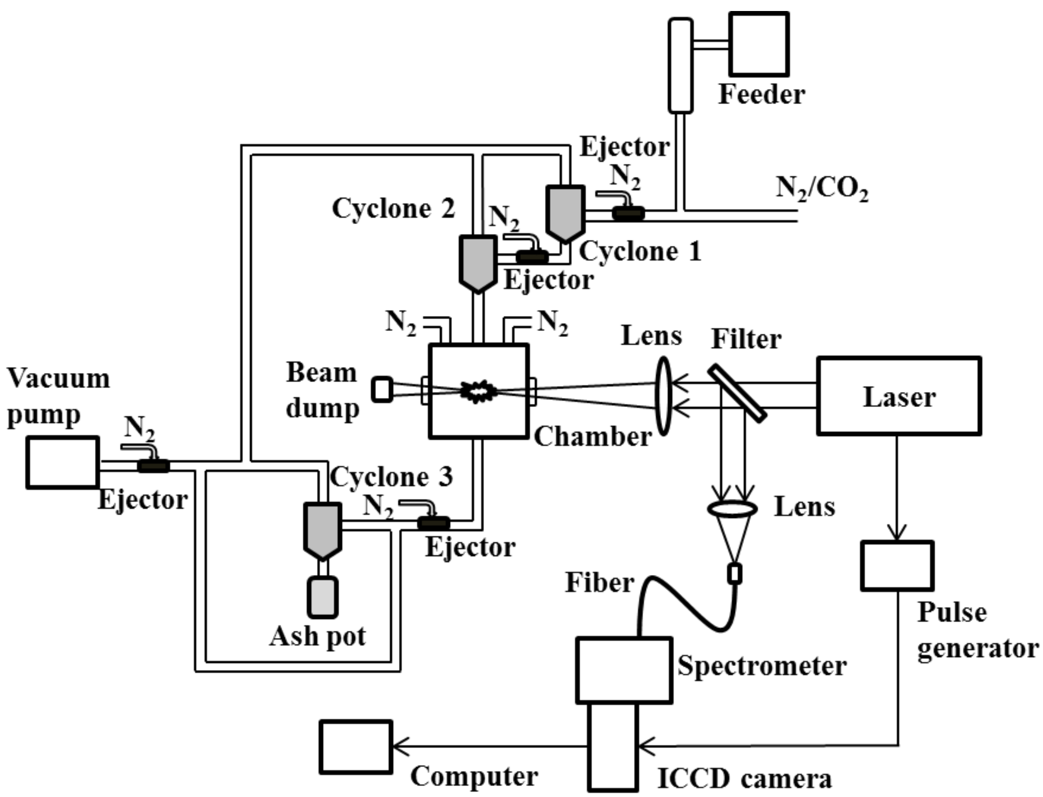

(a) Two-stage cyclone measurement system of fly ash flow

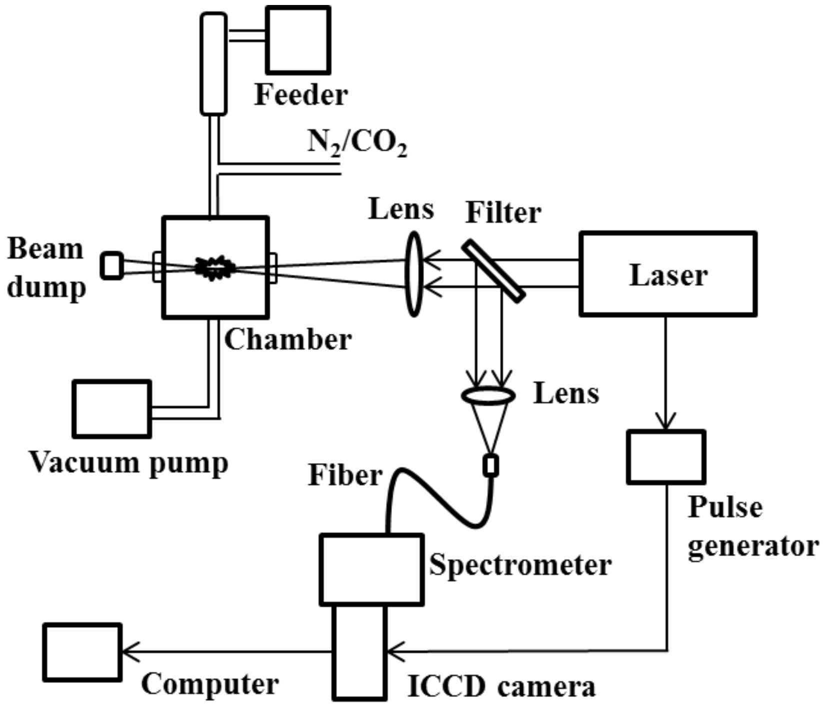

(b) Direct measurement system of fly ash flow

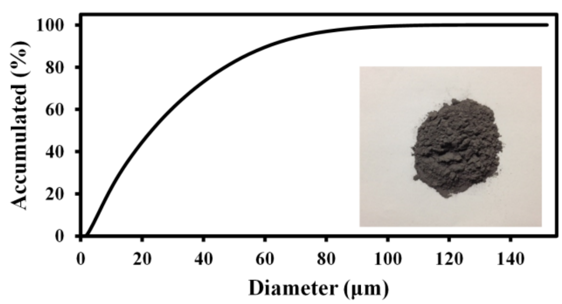

(c) Fly ash sample and particle size distribution

Figure 2. Schematic diagram of fly ash measurement using LIBS

Table 2. Contents of fly ash samples

number	Ash (%)										Unburned carbon(%)
	SiO_2	Al_2O_3	Fe_2O_3	K_2O	CaO	TiO_2	P_2O_5	SO_3	MgO	Na_2O	
1	54.0	19.5	4.5	0.9	2.3	1.0	0.2	1.8	1.0	0.2	14.0
2	45.0	25.1	6.2	2.5	0.8	1.1	0.2	0.2	0.6	0.3	17.3
3	49.6	18.0	4.1	0.8	2.1	0.9	0.2	1.6	0.9	0.2	21.0
4	39.0	26.4	5.7	0.4	1.3	0.8	0.4	0.5	0.6	0.7	23.1
5	37.4	25.9	6.3	0.4	1.4	0.8	0.4	0.5	0.6	0.8	24.9
6	46.0	16.6	3.8	0.8	2.0	0.9	0.2	1.5	0.9	0.2	26.8
7	38.1	13.8	3.2	0.6	1.7	0.7	0.1	1.3	0.7	0.2	39.3
8	29.4	10.6	2.4	0.5	1.3	0.6	0.1	1.0	0.6	0.1	53.2

The LIBS experimental setup for these two measurement systems was composed of lasers, beam focusing system, detection system and auxiliary devices. The beam from a Q-switched Nd:YAG laser (LOTIS TII, LS-2132UTF, 6ns, 10Hz) operating at 1064nm was focused into the measurement area using the lens with focus length of 200mm. In order to clarify the laser pulse-width effect, one small laser with the shorter pulse width of 1ns (Hamamatsu Photonics, Microchip Laser L12968-01) was also employed and operated at 1064nm in this study. The frequency of this small laser was adjusted by a function generator (Wave Factory 1941, Multifunction Synthesizer) to 10Hz. The laser power employed in this study was lower than that of gas breakdown threshold. The laser power of 1ns pulse-width laser was 9mJ/pulse. The laser power of 6ns pulse-width laser was 9mJ/pulse to compare the pulse width effect and 21mJ/pulse to discuss the two-stage cyclone measurement system features. The emission signals were separated from the laser path direction using a filter and focused into an optical fiber using the lens with focus length of 220mm. The emission signals were dispersed using a spectrometer (SOL instruments, NP250-2) and detected by an ICCD camera (Andor, iStar DH334T-18U-03) with the wavelength resolutions of 0.076nm/pixel and 0.012nm/pixel, and the wavelength ranges of 240nm-320nm and 247nm-255nm respectively. The spectrometer employed here with two channels can detect two wavelength ranges simultaneously when using different gratings of 600l/mm and 3600l/mm. The signal was accumulated by adjusting the exposure time and the spectra were averaged by multiple measurement.

4. Results and discussion

4.1 Identification of characteristic spectra

The different fly ash samples were measured using the experimental system shown in Fig. 2(a) under different delay time conditions. The fly ash samples with air as the buffer gas were introduced into the measurement chamber with two-stage cyclone measurement system. Fig. 3 shows the emission signals of fly ash with unburned carbon of 24.9% in delay time of 10ns using 1ns pulse-width laser without CO_2. The clear signals of fly ash contents were distinguished. The fly ash contains SiO_2, Al_2O_3, Fe_2O_3, CaO, unburned carbon and other materials. The main compositions were detected as shown in Fig. 3(a) at the wavelength resolution of 0.076nm/pixel. The characteristic emission spectra and their relevant parameters are listed in Table 3[43]. Fig. 3(b) shows the measured spectra of fly ash with clearly distinguishable C emission line at the wavelength resolution of 0.012nm/pixel. The emission spectra at the wavelength range of 247nm-255nm were discussed for the detection characteristics of C signal. The intensity of carbon emission line increased with the increase of unburned carbon content. The spectra emission intensity concerning species concentration also varied with different delay times, which means the alteration of plasma temperature. A detailed description was presented elsewhere[39-41].

Table 3. Upper level energy of detected species in fly ash[43]

Species	Upper energy (cm^{-1})	Wavelength (nm)
Si	39683.16-39955.05	250.69-252.85
Si	40991.88	288.16
Fe	38660.04-59663.46 (ion and atom)	259.66-263.13
Fe	36686.16-45289.80 (ion and atom)	274.20-275.63
Al	32435.45	308.21
Al	32436.8	309.27
Ca ion	56839.25	315.89
Ca ion	56839.25	318.13
C	61982.2	247.86
Mg1 ion	35760.88	279.55
Mg1 ion	35669.31	280.27
Mg2	35051.27	285.21

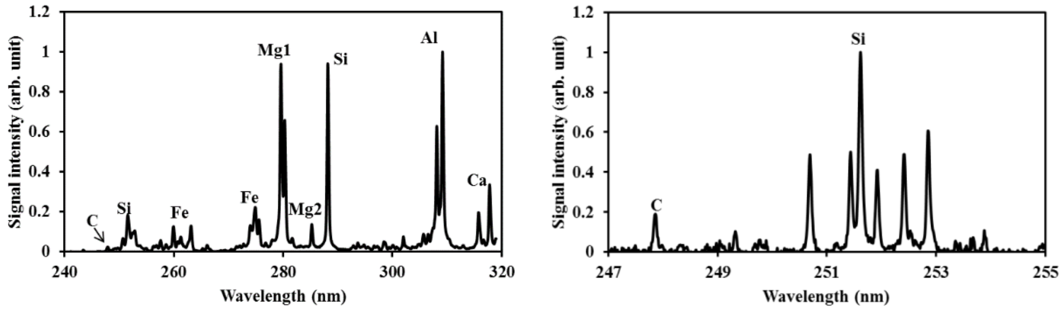

(a) Spectra at resolution of 0.076nm/pixel (b) Spectra at resolution of 0.012nm/pixel

Figure 3. Measured spectra of fly ash with unburned carbon of 24.9% using two-stage cyclone measurement system with 1ns pulse-width laser without CO_2

In the measurement of fly ash contents, CO_2 caused the spurious C signal for unburned carbon in LIBS spectra of fly ash[38]. The surrounding gas of CO_2 was also introduced into the measurement chamber to clarify the CO_2 effect on the emission intensity of C signal. The measured spectra varied with the sample and delay time, as well as surrounding gas and laser pulse width. The quantitative analysis method of fly ash contents was also studied under different conditions to quantitatively calculate the unburned carbon content of fly ash.

4.2 Effect of surrounding gas on fly ash contents

The CO_2 effect on unburned carbon content was rather sensitive to its concentration in surrounding gas. Therefore, the CO_2 effect was clarified to accurately evaluate unburned carbon in fly ash. In order to reduce the CO_2 effect on unburned carbon measurement, two different approaches were employed in this study, such as the short pulse-width laser of 1ns and the two-stage cyclone measurement system. The two-stage cyclone measurement system was employed to mainly reduce the surrounding CO_2 concentration efficiently. On the other hand, the laser-induced plasma processes were affected by the laser pulse width to reduce the surrounding gas breakdown.

4.2.1 Laser pulse-width effect

In the measurement of aerosols, the particles in surrounding gases can firstly become the core of plasma, which expands to the surrounding gases. Due to the different laser-induced plasma processes of particles and surrounding gases, the different pulse-width lasers were employed to verify the laser pulse-width effect on the laser-induced plasma processes. Two different pulse-width lasers including 1ns and 6ns were employed to measure the fly ash sample with unburned carbon of 24.9% for detection features comparison using the direct measurement system of fly ash flow under the same experimental conditions except for delay time. The delay time was different for different pulse-width lasers due to different plasma generation and development lifetime concerning the plasma state and signal quality. The measured spectra using 1ns pulse-width laser in delay time of 25ns were compared with that using 6ns pulse-width laser in delay time of 1000ns because of their similar plasma temperature. When the laser pulse width became shorter, the time of plasma reheating by laser pulse became shorter resulting in shorter plasma lifetime. More plasma was formed within the particles vapour due to the reduction of electron collision ionization for surrounding gas plasma by particle plasma. Therefore, when employing 1ns pulse-width laser, the breakdown rate of the surrounding gas decreased. The C signal from the CO_2 breakdown reduced. The fly ash flow breakdown processes including particle breakdown and surrounding gases breakdown, as well as the plasma states, were discussed by our group in detail presented elsewhere[42]. Fig.4(a) and Fig.4(b) show the measured results of fly ash with and without CO_2 using 6ns and 1ns pulse-width lasers, respectively. There was no significant change of the measured spectra with different CO_2 concentrations using 1ns pulse-width laser, as shown in Fig.4(b). However, C signal intensity increased obviously when introducing 3.8% CO_2 using 6ns pulse-width laser shown in Fig.4(a). This is because the CO_2 breakdown was induced by 6ns pulse-width laser and the fly ash particle plasma. The compared results indicated that CO_2 breakdown rate using 1ns pulse-width laser was much smaller than that using 6ns pulse-width laser. The CO_2 influence on the measurement of unburned carbon in fly ash can be obviously decreased when utilizing 1ns pulse-width laser to control the laser-induced particle plasma and surrounding gas plasma.

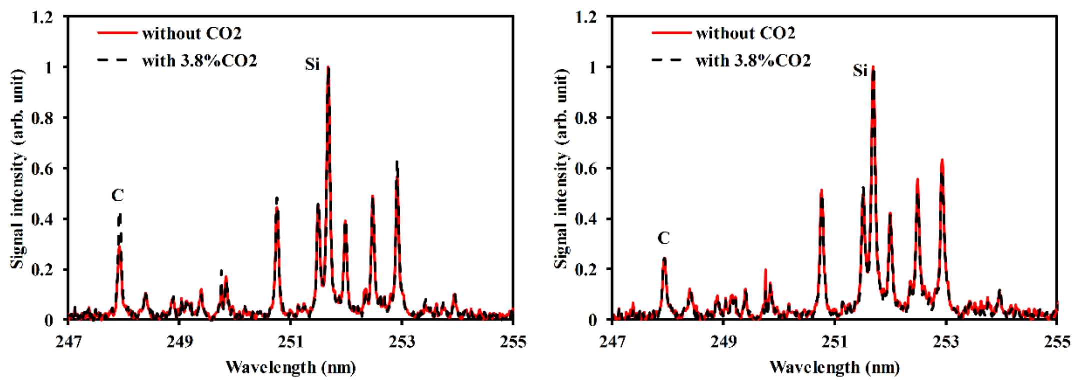

(a) Spectra using 6ns pulse-width laser (b) Spectra using 1ns pulse-width laser

Figure 4. Comparison of measured spectra of fly ash with unburned carbon of 24.9% under different CO_2 concentration conditions using direct measurement system with 1ns and 6ns pulse-width lasers

4.2.2 Two-stage cyclone measurement system

The CO_2 effect on unburned carbon measurement can also be decreased by reducing the CO_2 concentration in flue gases. The sampling of fly ash from gas duct using the cyclone measurement system in the coal-fired power plant is one of the effective methods to reduce the CO_2 effect. Due to the high concentration of CO_2 in exhaust, a cyclone measurement system has been employed to reduce the spurious C signal from CO_2 for unburned carbon measurement. However, the experimental conditions and parameters should be carefully controlled according to previous measurement system, such as the laser power[38]. Based on this previous study, a two-stage cyclone measurement system was constructed in the current experiment to reduce the influence of surrounding gases, especially CO_2, which concerning the measurement system. The fly ash sample with surrounding mixture gases were introduced to the two-stage cyclone measurement system.

The mixed sample was separated to fly ash particles and gases by cyclone 1. The recaptured fly ash particles with N_2 from ejector flowed into cyclone 2 to separate the fly ash particles efficiently. The recaptured fly ash particles from cyclone 2 were introduced to the measurement chamber. Therefore, the two-stage cyclone measurement system employed here can eliminate the CO_2 effect efficiently.

In order to verify the improved performance of the two-stage cyclone measurement system, the fly ash sample with unburned carbon of 24.9% was measured using the two-stage cyclone measurement system with 6ns pulse-width laser, as illustrated in Fig. 2(a). The fly ash was introduced into the measurement chamber with the surrounding gas of CO_2 in N_2 to compare the C content measurement results. When measuring the fly ash with different CO_2 concentrations using the two-stage cyclone measurement system, the measured spectra are showed in Fig. 5. When comparing the measured results without CO_2 and with 12.5% CO_2, the C signal showed the similar spectra with different CO_2 concentrations using the two-stage cyclone measurement system. However, C signal intensity increased obviously when introducing 3.8% CO_2 using the direct measurement system with 6ns pulse-width laser shown in Fig.4(a).

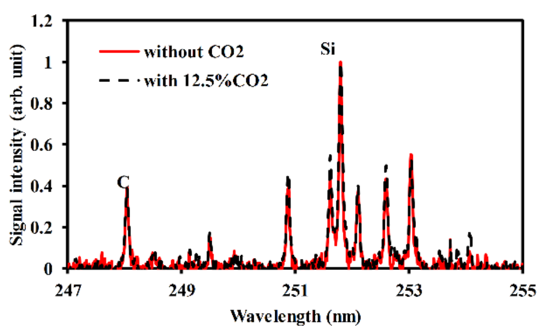

Figure 5. Measured spectra of fly ash with unburned carbon of 24.9% using two-stage cyclone measurement system with 6ns pulse-width laser under different CO_2 concentration conditions

The fly ash sample was measured using 6ns pulse-width laser with two-stage cyclone measurement system and direct measurement system respectively to compare the detection features. Fig. 6 shows the comparison of CO_2 effect on C signal with and without cyclone system using 6ns pulse-width laser under different CO_2 concentration conditions. C signal intensity increased rapidly without cyclone system when increasing the CO_2 concentration even if the CO_2 concentration was less than 1%. However, when employing the two-stage cyclone measurement system, C signal intensity became almost constant as increasing the CO_2 concentration. It is demonstrated the feasibility of this two-stage cyclone measurement system to eliminate the CO_2 effect for the actual power plant application.

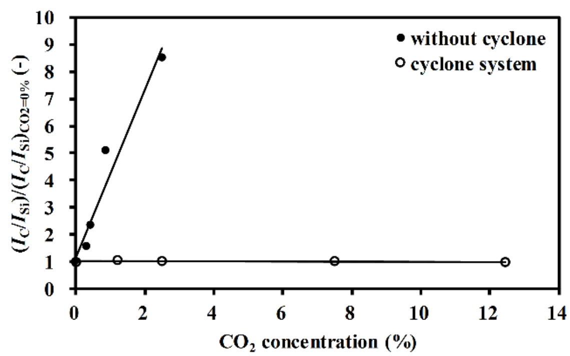

Figure 6. CO_2 effect on C signal with or without cyclone system using 6ns pulse-width laser

According to these measurement results, CO_2 effect on unburned carbon measurement in fly ash can be reduced efficiently when using 1ns pulse-width laser and the two-stage cyclone measurement system. In the actual power plants, the flue gas was not stable and constant. For example, the variations of pressure, flow rate and so on can affect the performance of two-stage cyclone measurement system. Some parameters of LIBS, especially laser power, can affect the laser-induced plasma processes of fly ash particle flow. Therefore, the combination of these two approaches can provide much better contents detection improvement for fly ash flow. Another merit is the system integration for the actual application in power plant due to the small size of 1ns pulse-width laser, which is a microchip laser with high durability and long lifetime.

4.3 Quantitative analysis of fly ash contents

The two-stage cyclone measurement system can separate fly ash particles and its surrounding gases effectively to reduce the influence of CO_2 on the unburned carbon content in fly ash. The CO_2 effect can also be reduced when using 1ns pulse-width laser. In this paper, the LIBS system for fly ash flow measurement using the two-stage cyclone measurement system with 1ns pulse-width laser was employed for quantitative analysis. The quantitative analysis method of fly ash contents was discussed using different fly ash samples. Fig. 7 shows the signal intensity ratio of I_C/I_{Si} variation with the unburned carbon contents for different fly ash samples. I_C/I_{Si} increased with the increase of unburned carbon content. Due to the temperature fluctuation of laser-induced plasma, I_C/I_{Si} was also fluctuated. Therefore, the plasma temperature correction is very essential to assure the quantitative analysis of LIBS measurement. The signal intensity ratios of I_{Al}/I_{Si}, I_{Fe}/I_{Si} and I_{Ca}/I_{Si} were also calculated to quantitatively analyze the carbon content in fly ash according to equation (2).

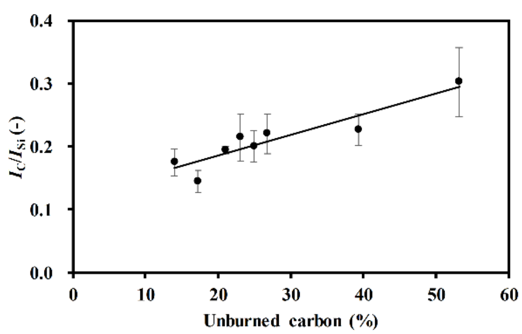

Figure 7. Unburned carbon dependence of I_C/I_{Si} using two-stage cyclone measurement system with 1ns pulse-width laser for different fly ash samples

A fly ash sample was measured to evaluate the plasma temperature correction factor under the experimental conditions using the two-stage cyclone measurement system. The emission intensity ratio of I_{Mg1}/I_{Mg2}, which is the same atom from different upper level energy, was employed as the plasma temperature indicator. One typical temperature correction curve and temperature correction result of I_C/I_{Si} are shown in Fig. 8. In Fig. 8(a) the emission intensity ratio of I_C/I_{Si} altered according to I_{Mg1}/I_{Mg2}, which means I_C/I_{Si} varied with the plasma temperature. When applying the plasma temperature correction scheme, the variation of I_C/I_{Si} became smaller under different plasma temperature conditions, as shown in Fig. 8(b). It can be confirmed the improved quantitative analysis. According to equation (2), the plasma temperature correction curves and correction results of other elements were also determined using the same method for quantitative calculation of carbon content. This plasma temperature correction method and factors were employed in this study to quantitatively calculate the contents in fly ash.

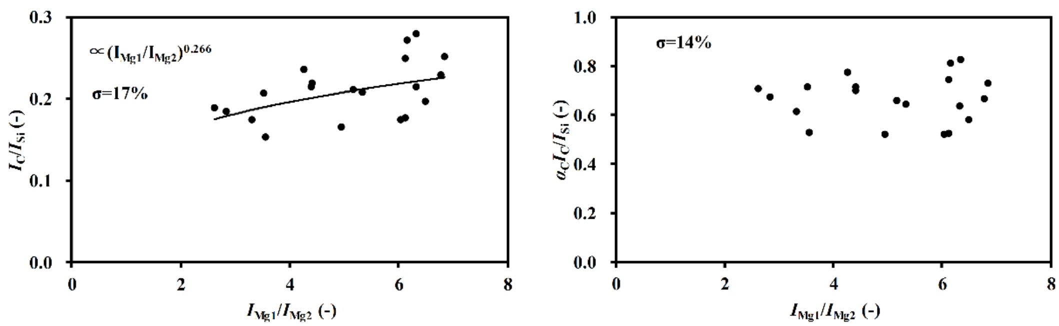

(a) Correction factor for I_C/I_{Si} (b) Correction result for I_C/I_{Si}

Figure 8. Plasma temperature correction curve and correction result of carbon signal using two-stage cyclone measurement system with 1ns pulse-width laser

The unburned carbon contents in different fly ash samples were measured by LIBS using the two-stage cyclone measurement system with 1ns pulse-width laser and quantitatively calculated with the temperature correction method. Fig. 9 shows the comparison of unburned carbon content in different fly ash samples measured using the chemical analysis method and LIBS technique. The measurement results of unburned carbon in fly ash using LIBS were consistent with the chemical analysis results with R^2=0.9052 and RMSEP(root-mean-square error of prediction)=3.9% in the measurement range of 14.0-53.2% unburned carbon. One reason for error was that the fly ash particle flow was measured in this study. The laser-induced plasma was not uniform and the measured signals, such as unburned carbon, fluctuated due to the un-uniformity of the employed fly ash particle flow. The detection limit of unburned carbon was also evaluated by 100shots(10seconds) to be 0.65% with S/N(signal to noise ratio)=1. Except for the unburned carbon content, other main components of fly ash can also be analyzed using this temperature correction method. These results show that the quantitative capability of LIBS for aerosol measurement can be improved using the plasma temperature correction method.

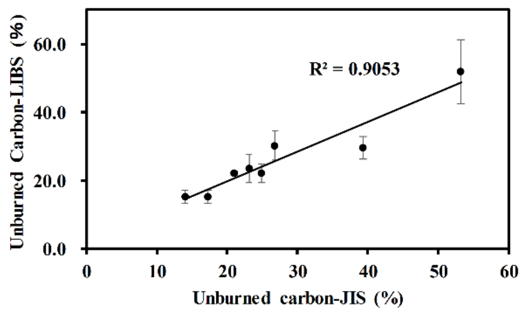

Figure 9. Comparison of unburned carbon contents measurement between standard method and LIBS using 1ns pulse-width laser

5. Conclusion

Particle measurement is not only benefit to industrial processes, but also important for the environmental protection and human health aspects. The content measurement of fly ash samples in real time was studied using LIBS in this study. A two-stage cyclone measurement system was constructed and 1ns pulse-width laser was also employed to measure the fly ash contents, especially the unburned carbon in fly ash. The main compositions of fly ash and target element can be detected at the wavelength resolutions of 0.076nm/pixel and 0.012nm/pixel simultaneously.

1. When employing 1ns pulse-width laser, the measured spectra of fly ash with different CO_2 concentrations showed the similar spectra. The CO_2 effect on unburned carbon signal can be reduced compared to that using 6ns pulse-width laser due to the laser pulse-width influence on the

laser-induced plasma processes of particles and surrounding gases. It is also benefit for the system integration because of the small size of 1ns pulse-width laser with high durability and long lifetime.

2. The influence of surrounding gases, especially CO_2 effect on unburned carbon measurement in fly ash, was discussed when comparing the measured results using the direct measurement system and two-stage cyclone measurement system with different CO_2 concentrations. The CO_2 effect can be eliminated efficiently when employing the constructed two-stage cyclone measurement system to reduce the CO_2 concentration. The C signal showed the similar spectra with different CO_2 concentrations.

3. In order to improve the quantitative analysis ability, the temperature correction method was proposed and applied when employing the intensity ratio of the emission pair from magnesium as a plasma temperature indicator. The plasma temperature correction factor was evaluated under the experimental conditions. The measured results of unburned carbon in fly ash using LIBS technique were consistent with the chemical analysis results.

These achieved results demonstrated the feasibility of the combination method of 1ns pulse-width laser and two-stage cyclone measurement system with temperature correction method to improve LIBS detection ability for the content measurement of fly ash in actual power plants.

AUTHOR INFORMATION

Corresponding Author

* Yoshihiro Deguchi, ydeguchi@tokushima-u.ac.jp, TEL: (+81)-88-656-7375, FAX: (+81)-88-656-9082

Acknowledge

This work was supported by National Natural Science Foundation of China (No. 51506171), the National Key Basic Research Development Plan (No. 2015CB251504) and Postdoctoral Science Foundation of China (No. 2015M582655).

Reference

[1] Liu P.Y.; Gao J.J.; Zhang H.; Zhang D.L.; Wu Y.X.; Zhang M.; Lu J.F. *Fuel Process. Technol.* **2017**, 158, 172-179.

[2] Li J.; Jankowski R.; Kotecki M.; Yang W.H.; Szewczyk D.; Brzdekiewicz A.; Blasiak W. *Energy Fuels* **2012**, 26, 926-937.

[3] Burris S.C.; Li D.; Riley J.T. *Energy Fuels* **2005**, 19, 1493-1502.

[4] Ma H.H.; Zhou L.; Ma S.X.; Yang S.L.; Zhao Y.; Zhang W.; Chew J.W. *Fuel Process. Technol.* **2018**, 179, 277-284.

[5] Singh L.P.; Ali D.; Tyagi I.; Sharma U.; Singh R.; Hou P. *Constr. Build. Mater.* **2019**, 194, 205-215.

[6] Dindi A.; Quang D.V.; Vega L.F.; Nashef E.; Abu-Zahra M.R.M. *J. CO2 Util.* **2019**, 29, 82-102.

[7] Ge J.C.; Kim J.Y.; Yoon S.K.; Choi N.J. *Fuel* **2019**, 237, 236-244.

[8] Asl S.M.H.; Javadian H.; Khavarpour M.; Belviso C.; Taghavi M.; Maghsudi M. *J. Cleaner Prod.* **2019**, 208, 1131-1147.

[9] Temuujin J.; Surenjav E.; Ruescher C.H.; Vahlbruch J. *Chemosphere* **2019**, 216, 866-882.

[10] Miziolek A.W.; Palleschi V.; Schechter I. *Laser-Induced Breakdown Spectroscopy (LIBS): Fundamentals and Applications*; Cambridge University Press: Cambridge, **2006**.

[11] Deguchi Y. *Industrial Applications of Laser Diagnostics*; Taylor & Francis Group, CRC Press: New York, 2011.

[12] Hahn D.W.; Omenetto N. *Appl. Spectrosc.* **2010**, 64(12), 335A-366A.

[13] Hahn D.W.; Omenetto N. *Appl. Spectrosc.* **2012**, 66(4), 347-419.

[14] Radziemski L.J.; Cremers D.A. *Handbook of Laser-Induced Breakdown Spectroscopy*; John Wiley & Sons, Ltd: Chichester, England, 2006.

[15] Noll R. *Laser-Induced Breakdown Spectroscopy: Fundamentals and Applications*; Springer: Germany, 2012.

[16] Wang Q.Q.; Liu K.; Zhao H.; Ge C.H.; Huang Z.W. *Frontiers of Physics* **2012**, 7(6), 701-707.

[17] Zhang Y.Y.; Xiong G.; Li S.Q.; Dong Z. Z.; Buckley S.G.; Tse S.D. *Combust. Flame* **2013**, 160, 725-733.

[18] Yi R.X.; Guo L.B.; Zou X.H.; Li J.M.; Hao Z.Q.; Yang X.Y.; Li X.Y.; Zeng X.Y.; Lu Y.F. *Opt. Express* **2016**, 24(3), 2607-2618.

[19] Sheta S.; Afgan M.S.; Hou Z.Y.; Yao S.C.; Zhang L.; Li Z.; Wang Z. *J. Anal. At. Spectrom.* **2019**, DOI: 10.1039/c9ja00016j.

[20] Wallis F.J.; Chadwick B.L.; Morrison R.J.S. *Appl. Spectrosc.* **2000**, 54, 1231-1235.

[21] Mateo M.P.; Nicolas G.; Yañez A. *Appl. Surf. Sci.* **2007**, 254, 868-872.

[22] Gaft M.; Dvir E.; Modiano H.; Schone U. *Spectrochim. Acta, Part B* **2008**, 63, 1177-1182.

[23] Ctvrtnickova T.; Mateo M.P.; Yañez A.; Nicolas G. *Spectrochim. Acta, Part B* **2009**, 64, 1093-1097.

[24] Ctvrtnickova T.; Mateo M.P.; Yañez A.; Nicolas G. *Spectrochim. Acta, Part B* **2010**, 65, 734-737.

[25] Haider A.F.M.Y.; Rony M.A.; Abedin K.M. *Energy Fuels* **2013**, 27, 3725-3729.

[26] He Y.; Zhu J.J.; Li B.; Wang Z.H.; Li Z.S.; Alden M.; Cen K.F. *Energy Fuels* **2013**, 27, 1123-1130.

[27] Romero C.E.; Saro R.D.; Craparo J.; Weisberg A.; Moreno R.; Yao Z. *Energy Fuels* **2010**, 24, 510-517.

[28] Lu Z.M.; Mo J.H.; Yao S.C.; Zhao J.B.; Lu J.D. *Energy Fuels* **2017**, 31, 3849-3855.

[29] Yao S.C.; Zhao J.B.; Xu J.L.; Lu Z.M.; Lu J. D. *J. Anal. At. Spectrom.* **2017**, 32, 766-772.

[30] Yuan T.B.; Wang Z.; Li L.Z.; Hou Z.Y.; Li Z.; Ni W.D. *Appl. Opt.* **2012**, 51, B22-B29.

[31] Yin W.B.; Zhang L.; Dong L.; Ma W.G.; Jia S.T. *Appl. Spectrosc.* **2009**, 63(8), 865-872.

[32] Zhang L.; Gong Y.; Li Y.F.; Wang X.; Fan J.J.; Dong L.; Ma W. G.; Yin W.B.; Jia S.T. *Spectrochim. Acta, Part B* **2015**, 113, 167-173.

[33] Zhang L.; Ma W.G.; Dong L.; Yan X.J.; Hu Z.Y.; Li Z.X.; Zhang Y.Z.; Wang L.; Yin W.B.; Jia S.T. *Appl. Spectrosc.* **2011**, 65(7), 790-796.

[34] Yao S.C.; Shen Y.L.; Yin K.J.; Pan G.; Lu J.D. *Energy Fuels* **2015**, 29, 1257-1263.

[35] Yao S.C.; Zhang L.F.; Xu J.L.; Yu Z.Y.; Lu Z.M. *Energy Fuels* **2017**, 31, 12093-12099.

[36] Yao S.C.; Xu J.L. Zhao J.B.; Bai K.J.; Lu J.D.; Lu Z.M. *Energy Fuels* **2017**, 31, 4681-4686.

[37] Noda M.; Deguchi Y.; Iwasaki S.; Yoshikawa N. *Spectrochim. Acta, Part B* **2002**, 57, 701-709.

[38] Kurihara, M.; Ikeda K.; Izawa Y.; Deguchi Y.; Tarui H. *Appl. Opt.* **2003**, 42, 6159-6165.

[39] Wang Z.Z.; Deguchi Y.; Kuwahara M.; Taira T.; Zhang X.B.; Yan J.J.; Liu J.P.; Watanabe H.; Kurose R. *Spectrochim. Acta, Part B* **2013**, 87, 130-138.

[40] Wang Z.Z.; Deguchi Y.; Watanabe H.; Kurose R.; Yan J.J.; Liu J.P. *J. Flow Control, Meas. Visualization* **2015**, 3, 10-21.

[41] Wang Z.Z.; Deguchi Y.; Katsumori S.; Ikutomo A.; Yan J.J.; Liu J.P.; Tainaka K.; Tanno K.; Watanabe H.; Kurose R. *Spectroscopy-Laser and Optics Interface* **2016**, 31, 22-35.

[42] Liu R.W.; Deguchi Y.; Nan W.G.; Hu R.M.; Wang Z.Z.; Fujita Y.; Tanaka S.; Tainaka K., Tanno K.; Watanabe H.; Liu J.P.; Yan J.J. *Adv. Powder Technol.* **2019**, 30, 1210-1218.

[43] Kramida, A.; Ralchenko, Y.; Reader, J.; NIST ASD Team. *NIST Atomic Spectra Database* (ver. 5.6.1), [Online]. Available: https://physics.nist.gov/asd. National Institute of Standards and Technology, Gaithersburg, MD. **2018**.